The American Journal of Pathology, Vol. 185, No. 3, March 2015

The American Journal of PATHOLOGY
ajp.amjpathol.org

See related Commentary on page 610

CARDIOVASCULAR, PULMONARY, AND RENAL PATHOLOGY

A Novel Nonhuman Primate Model of Cigarette Smoke–Induced Airway Disease

Francesca Polverino,*†‡ Melanie Doyle-Eisele,† Jacob McDonald,† Julie A. Wilder,† Christopher Royer,† Maria Laucho-Contreras,*† Emer M. Kelly,* Miguel Divo,*† Victor Pinto-Plata,*† Joe Mauderly,† Bartolome R. Celli,*† Yohannes Tesfaigzi,† and Caroline A. Owen*†

From the Division of Pulmonary and Critical Care Medicine, Brigham and Women's Hospital, Harvard Medical School, Boston, Massachusetts; The Lovelace Respiratory Research Institute,† Albuquerque, New Mexico; and the Pulmonary Department,‡ University of Parma, Parma, Italy*

Accepted for publication November 4, 2014.

Address correspondence to Caroline A. Owen, M.D., Ph.D., Division of Pulmonary and Critical Care Medicine, Brigham and Women's Hospital, Room 855B, Harvard Institutes of Medicine Bldg, 77 Ave Louis Pasteur, Boston, MA 02115; or Yohannes Tesfaigzi, Ph.D., COPD Program, Lovelace Respiratory Research Institute, 2425 Ridgecrest Dr SE, Albuquerque, NM 87108. E-mail: cowen@rics.bwh.harvard.edu or ytesfaig@lrri.org.

Small animal models of chronic obstructive pulmonary disease (COPD) have several limitations for identifying new therapeutic targets and biomarkers for human COPD. These include a pulmonary anatomy that differs from humans, the limited airway pathologies and lymphoid aggregates that develop in smoke-exposed mice, and the challenges associated with serial biological sampling. Thus, we assessed the utility of cigarette smoke (CS)–exposed cynomolgus macaque as a nonhuman primate (NHP) large animal model of COPD. Twenty-eight NHPs were exposed to air or CS 5 days per week for up to 12 weeks. Bronchoalveolar lavage and pulmonary function tests were performed at intervals. After 12 weeks, we measured airway pathologies, pulmonary inflammation, and airspace enlargement. CS-exposed NHPs developed robust mucus metaplasia, submucosal gland hypertrophy and hyperplasia, airway inflammation, peribronchial fibrosis, and increases in bronchial lymphoid aggregates. Although CS-exposed NHPs did not develop emphysema over the study time, they exhibited pathologies that precede emphysema development, including increases in the following: i) matrix metalloproteinase-9 and proinflammatory mediator levels in bronchoalveolar lavage fluid, ii) lung parenchymal leukocyte counts and lymphoid aggregates, iii) lung oxidative stress levels, and iv) alveolar septal cell apoptosis. CS-exposed NHPs can be used as a model of airway disease occurring in COPD patients. Unlike rodents, NHPs can safely undergo longitudinal sampling, which could be useful for assessing novel biomarkers or therapeutics for COPD. *(Am J Pathol 2015, 185: 741–755; http://dx.doi.org/10.1016/j.ajpath.2014.11.006)*

Chronic obstructive pulmonary disease (COPD) is a major cause of morbidity and mortality worldwide.[1,2] COPD is characterized by airflow limitation that is not fully reversible and associated with abnormal pulmonary inflammation induced by noxious particles and gases most commonly present in cigarette smoke (CS).

Mice are widely used to investigate the biological pathways that contribute to lung pathologies occurring in CS-induced COPD and to test the efficacy of novel therapies for COPD.[3] Mice exposed to CS for 6 months exhibit some features of human COPD, including chronic pulmonary inflammation, modest airspace enlargement, and mild small airway fibrosis.[3] The use of mice to model COPD has several advantages, including the following: i) opportunities for genetic manipulation and the availability of molecular reagents to probe changes in pathways *in vivo*, ii) rapid breeding rate, and iii) small size, which is advantageous for dosing expensive drugs. However, murine COPD models have several limitations. In contrast to humans, mice lack bronchial submucosal glands, clearly defined respiratory bronchioles, and a distinct lobular architecture.[4] Mice also have a monopodial airway branching pattern, rather than the

Supported by the Brigham and Women's Hospital-Lovelace Respiratory Research Institute Research Consortium (Y.T. and C.A.O.), NIH grants P50 HL107165-01 (B.R.C. and Y.T.), P01 HL105339 (B.R.C. and C.A.O.), PO1 HL114501 (B.R.C. and C.A.O.), HL68111 (Y.T.), ES015482 (Y.T.), RO1 AI111475 (C.A.O.), and R21 HL111835 (C.A.O.), and The Flight Attendant Medical Research Institute grant CIA#123046 (C.A.O. and B.R.C.).

Y.T. and C.A.O. contributed equally to this work as senior authors.

Disclosures: None declared.

http://dx.doi.org/10.1016/j.ajpath.2014.11.006

dichotomous pattern found in humans.[5] Moreover, there are differences in the innate and adaptive immune systems[6] and in the expressed profiles of matrix metalloproteinases (MMPs) in humans versus mice.[7] In mice, it is also challenging to perform serial sampling in blood or lungs to measure biomarkers of CS-induced lung injury or responses to therapies. Furthermore, mice do not develop robust airway pathologies, including mucus hypersecretion and small airway fibrosis, when exposed chronically to CS. Also, several therapies, including an anti-tumor necrosis factor α antibody,[8] roflumilast,[9] simvastatin,[10] and antioxidants[11] that have effectively treated emphysema in mice, were substantially less effective when tested in COPD patients,[7,12–14] raising the issue about the utility of smoke-exposed mice for testing novel therapeutics for the human disease. Smoke-exposed guinea pigs have been used as an alternative to mice as a small animal model of COPD but have several disadvantages, including the lack of availability of commercially available reagents for interrogating pathways in guinea pigs.[15] Thus, there is a need for alternative animal models that better recapitulate the physiological and pathological changes occurring in the lungs of human COPD patients.

Other models for studying disease pathogenesis and preclinical testing of pharmaceuticals have been established in larger animals.[5,16] Among these, nonhuman primates (NHPs) have great potential because their pulmonary anatomy and immune system are similar to those of humans. Also, NHP and human proteins have a high degree of homology, and molecular reagents used in studies of human samples often can be used to probe pathways in NHP samples.[17]

When challenged with allergens, NHPs develop allergic airway inflammation, hyperresponsiveness, and extensive airway remodeling pathologies resembling that which occurs in human asthmatics.[5] In addition, exposing NHPs to ozone produces a persistent chronic respiratory bronchiolitis[18] similar to that occurring in human smokers.[19] However, to our knowledge, there have been no prior reports of the effects of CS exposure on the NHP lung. We hypothesized that when exposed to CS, NHPs would develop pathological and functional changes in their lungs similar to those occurring in the airways of COPD patients. To test this hypothesis, we evaluated the airway and alveolar pathologies and lung physiology in cynomolgus macaques (*Macaca fascicularis*) exposed to air or CS for up to 12 weeks. Some results have been presented in abstract form.[20]

Materials and Methods

Animals

All cynomolgus macaque (*M. fascicularis*) NHPs were female, with an average age of 11 years ± SD 1 year and an average weight of 3.2 ± SD 0.37 kg. All animals studied were female because women who smoke have a higher risk of developing COPD than men regardless of smoking level or intensity.[21] Also, female mice develop more severe airspace enlargement than male mice when exposed to the same dose of CS for the same duration.[22]

Care of the animals complied with the regulations of the US Department of Agriculture guidelines on the protection of animals and the NIH's *Guide for the Care and Use of Laboratory Animals*[23] used for scientific purposes. All experiments conducted on NHPs were approved by our Institutional Animal Care and Use Committee. The NHPs were socially housed (up to two animals per cage) in the Primate Facility at the Lovelace Respiratory Research Institute (Albuquerque, NM), in accordance with the Guide for Laboratory Animal Practice under the Association for the Assessment and Accreditation for Laboratory Animal Care International–approved animal environmental conditions. The animal facility maintained a 12-hour light cycle. NHPs were exposed to 100% freshly filtered air with 10 to 15 air changes per hour in the control and CS exposure group before initiating the exposures. Room temperature and relative humidity were maintained according to the *Guide for the Care and Use of Laboratory Animals*.[23] NHPs were observed a minimum of twice daily for any sign of illness. NHPs were fed twice daily with water available at all times. Animals were weighed during each physical examination or collection period until necropsy.

CS Exposures

NHPs were placed into H2000 whole body exposure chambers and exposed to CS [250 mg/m^3 total suspended particulate matter (TPM)] for 6 hours per day, 5 days per week, because this exposure protocol is most commonly used to model COPD in small animals, including mice.[24–26] We used an initial CS concentration of 100 mg/m^3 TPM to acclimatize the animals to CS, and then we increased it to the target concentration of 250 mg/m^3 TPM during the first 5 exposure days. These target CS exposure levels (100 and 250 mg/m^3 TPM) were selected to simulate a heavy human smoking pattern. For a 3000-g primate inhaling an average volume of 800 mL/minute, a pulmonary TPM deposition of 20%, and a lung weight of 10 g, the weekly deposition of smoke particles would be approximately 2.9 or 7.2 TPM deposited per gram of lung per week, as was calculated previously.[27] Assuming that a human smoker with 20 cigarettes per day over 1 week will have 1.8 mg TPM deposited per gram of lung per week, the 100 and 250 mg/m^3 TPM CS dose for NHPs is similar to that of humans smoking approximately 1.8 or 4 packs per day, respectively.

Time Points for Serial Sampling

Two different studies were performed. In the first experiment, NHPs were exposed to CS ($n = 8$) or air ($n = 4$) for 4 weeks in H2000 whole-body inhalation chambers for 6 hours per day, 5 days per week, to determine whether this exposure results in significant increases in pulmonary inflammation and/or mucus metaplasia in airway epithelia.

Physical examination and bronchoalveolar lavage (BAL) were performed at baseline before CS exposures were initiated and after 1 and 4 weeks, and lung tissue was obtained at necropsy (Table 1).

In the second experiment, NHPs were exposed to CS ($n = 8$) or air ($n = 8$) for 12 weeks in H2000 whole-body inhalation chambers for 6 hours per day, 5 days per week, to determine whether airway and/or airspace pathologies develop in the animals. Physical examination, pulmonary function tests (PFTs), and BAL were performed at baseline and after 4 and 12 weeks, and lung tissue was obtained at necropsy (Table 1). Exposures >12 weeks were not feasible because of the high costs associated with husbandry, performing the exposures, and sample collections.

PFT

PFT was performed on NHPs exposed to air or CS for 12 weeks ($n = 8$ animals per group) using a whole-body flow plethysmography constructed and operated as described previously for dogs.[28] The animals were anesthetized with 2% to 3% isoflurane and intubated, an esophageal catheter was inserted, and the animals were placed supine in the plethysmograph. The endotracheal tube was attached to an airway port, and the distal end of the esophageal catheter was passed through a small opening located near the airway port. The esophageal catheter was connected to a differential pressure transducer that was vented to the airway for measurement of transpulmonary pressure. A valve system allowed the airway to be connected to positive and negative pressure reservoirs for induction of inspiration and expiration. The data collection program was initiated, and the depth of the esophageal catheter was adjusted to maximize the transpulmonary pressure trace. Anesthesia was maintained at a light surgical plane for the duration of testing. During apnea induced by brief hyperventilation, the airway was connected to the positive pressure reservoir through a valve that provided a slow inspiration to total lung capacity, defined as a transpulmonary pressure of 30 cm H_2O. The pressure-volume trace was recorded during quasistatic expiration (5 seconds), and the quasistatic chord compliance was measured as the slope between 10 cm H_2O and functional residual capacity (relaxed lung volume). After a period of spontaneous respiration, the hyperventilation-inspiration sequence was repeated, followed by evacuation of the lung to the negative pressure reservoir without intentional limitation of flow. The forced vital capacity, the percentage of forced vital capacity exhaled in 0.1 seconds, and the peak expiratory flow were measured during this forced expiration.

Table 1 Design of the 4- and 12-Week CS versus Air Exposure Experiment

Exposure time points	Procedures performed
4-Week exposure	
Baseline	Physical examination, (BAL) on 12 NHPs
1 Week	All animals: physical examination and BAL on eight CS-exposed and four air-exposed NHPs
4 Weeks	End CS exposures on CS animals All animals: physical examination, BAL, and lung tissue collection on eight CS-exposed and four air-exposed NHPs
12-Week exposure	
Baseline	Physical examination, BAL, and PFTs on 16 NHPs
4 Weeks	All animals: physical examination, BAL, and PFTs on eight CS-exposed and eight air-exposed NHPs
12 Weeks	End CS exposures on CS animals All animals: physical examination, BAL, PFTs, and lung tissue collection on eight CS-exposed and eight air-exposed NHPs

BAL, bronchoalveolar lavage; CS, cigarette smoke; NHP, nonhuman primate; PFT, pulmonary function test.

BAL

Bronchoscopy, followed by BAL, was performed at baseline and after 1, 4, and/or 12 weeks of exposure to CS or air (Table 1). Animals were sedated with 5 to 10 mg/kg ketamine (delivered by the i.m. route) and anesthetized with inhaled isoflurane delivered using a mask. An endotracheal tube of an appropriate size for the animal was placed into the animal's trachea. A bronchoscope (model BF-3C40; Olympus America Inc., Melville, NY) was maneuvered through the endotracheal tube and wedged in approximately a fourth- to sixth-generation airway in the right diaphragmatic lung lobe. Two 10-mL aliquots of sterile USP-grade endotoxin-free saline were instilled and aspirated in succession, followed by further aspiration with an empty syringe to recover as much BAL fluid (BALF) as possible, which was frozen to −80°C for subsequent analyses.

Pulmonary Inflammation Measured in BAL Samples

All leukocytes, macrophages, polymorphonuclear neutrophils (PMNs), and lymphocytes were counted in BAL samples from air- and CS-exposed NHPs (four air- and eight CS-exposed NHPs in the 4-week exposure experiment and eight NHPs per group in the 12-week exposure experiment). IL-6, chemokine (C-X-C motif) ligand 8 (CXCL8), and chemokine (C-X-C motif) ligand 2 (CCL2) levels were measured in BALF from air- and CS-exposed NHPs (eight animals per group) using the Milliplex multi-analyte panels NHP cytokine Luminex multiplex assay (EMD Millipore, Billerica, MA). MMP-9 levels were measured in BALF samples using a human Duoset MMP-9 enzyme-linked immunosorbent assay kit (R&D Systems, Minneapolis, MN). We used Western blot analysis to measure MMP-12 levels in BALF samples from NHPs exposed to air ($n = 3$) or CS for 4 weeks ($n = 3$) and 12 weeks ($n = 3$), and in radioimmunoprecipitation assay extracts of BAL leukocytes from

NHPs exposed to air ($n = 7$) or CS for 4 weeks ($n = 4$) or 12 weeks ($n = 7$). Briefly, equal amounts of total protein (30 μg) were reduced by adding Laemmli sample buffer containing dithiothreitol and heating to 90°C for 5 minutes. Proteins in the samples were separated on 12% SDS-polyacrylamide gels for 4 hours at 90 V. Proteins were then transferred to polyvinylidene difluoride membranes, blocked in phosphate-buffered saline (PBS) containing 3% nonfat milk and 0.1% Tween-20 for 2 hours at room temperature, and incubated overnight with rabbit anti–MMP-12 IgG (diluted 1:100; Abcam, Cambridge, MA) and rabbit anti-vinculin IgG (diluted 1:1000; Abcam) as a loading control. After washing the membranes with PBS containing 0.1% Tween-20, the membranes were incubated with horseradish peroxidase–conjugated goat anti-rabbit IgG (diluted 1:3000; BioRad, Hercules, CA) for 2 hours at room temperature, and developed using a chemiluminescence substrate (Thermo Scientific, Pittsburgh, PA) following the manufacturer's directions. The membranes were exposed to a charge-coupled device camera for 30 minutes (BioRad). Signals were quantified using densitometry with Scion Image software for Windows Beta 4.0.2 (Scion Corporation, Bethesda, MD), and MMP-12 signals were corrected for vinculin signals.

Pulmonary Inflammation Measured in Lung Sections

To identify the inflammatory cell subsets that were recruited into the lung parenchyma of CS-exposed NHPs, we performed immunofluorescence staining for markers of macrophages and polymorphonuclear neutrophils in formalin-fixed lung sections from NHPs exposed to air or CS for 12 weeks ($n = 5$ per group). Briefly, the lung sections were deparaffinized, and antigen (Ag) retrieval was performed by heating the slides in a microwave in 0.01 mol/L sodium citrate and 2 mmol/L citrate buffer (pH 6.0). The sections were incubated for 1 hour at 37°C with either a murine IgG to human myeloperoxidase (diluted 1:20) as a marker of neutrophils or a rabbit anti-human CD68 IgG (diluted 1:20) as a marker of macrophages. Isotype-matched nonimmune murine and rabbit IgGs were used as controls. After washing the lung sections with PBS, the sections were incubated at 37°C for 1 hour with Alexa 488–conjugated goat anti-murine $F(ab')^2$ diluted 1:100 or Alexa 488–conjugated goat anti-rabbit $F(ab')^2$ diluted 1:100. Sections were then washed in PBS, and nuclei were counterstained with DAPI. Images of the stained lung sections were analyzed using a confocal microscope (Leica Microsystems, Buffalo Grove, IL). Confocal micrographs were recorded under a fluorescence imaging mode in which cells were exposed to 488-nm light attenuated by an acustotunable optical filter.[29]

Lymphoid Aggregates

To quantify the number of lymphoid aggregates present in the airways and lung parenchyma, paraffin-embedded sections (5 μm thick) of lungs from NHPs exposed to air or CS for 12 weeks (seven animals per group) were stained with hematoxylin and eosin. For each NHP, 30 high-magnification fields were counted in a randomized manner using a Leica epifluorescence microscope (Leica Microsystems). We evaluated all lymphoid aggregates containing >40 contiguous mononuclear cells. Data were expressed as the number of parenchymal, peribronchial, and perivascular lymphoid aggregates/mm^2 of tissue examined in 30 randomly acquired images per animal.

To identify B- and T-lymphocyte subsets within the lymphoid aggregates, we performed triple-immunofluorescence staining of lung sections from NHPs exposed to air or CS for 12 weeks ($n = 5$ lung sections per group). Briefly, the lung sections were deparaffinized, and Ag retrieval was performed by heating the slides in a microwave in 0.01 mol/L sodium citrate and 2 mmol/L citrate buffer (pH 6.0). The sections were incubated for 2 hours at 37°C with murine anti-human CD4 IgG (diluted 1:50; Abcam), then for 1 hour at 37°C with rat anti-human CD8 IgG (diluted 1:100; Abcam), and then overnight at 4°C with rabbit anti-human CD20 IgG (diluted 1:100; Abcam). After washing the lung sections with PBS, the sections were incubated at 37°C for 1 hour with Alexa Cy5-conjugated goat anti-murine IgG (diluted 1:100), Alexa 546–conjugated goat anti-rat IgG (diluted 1:100), and Alexa 488–conjugated F(ab')2 fragment of goat anti-rabbit IgG (diluted 1:100). Sections were then washed in PBS, and nuclei were counterstained with DAPI. Images of the stained lung sections were analyzed using a confocal microscope (Leica Microsystems). Confocal micrographs were recorded under fluorescence imaging mode in which cells were exposed to 488-, 570-, and 670-nm light attenuated by an acustotunable optical filter.[29]

Mucus Metaplasia

Lung sections from seven NHPs exposed to air and eight NHPs exposed to CS for 4 or 12 weeks were stained with periodic acid–Schiff stain using commercial kits (Sigma-Aldrich, St. Louis, MO) following the manufacturer's instructions. We also immunostained lung sections from NHPs that were exposed to air ($n = 6$) or CS ($n = 10$) for 4 or 12 weeks for MUC5AC. Briefly, the lung sections were deparaffinized, and Ag retrieval was performed by heating the slides in a microwave in 0.01 mol/L sodium citrate and 2 mmol/L citric acid buffer citrate buffer (pH 6.0). Sections were incubated with blocking medium (PBS containing 1% normal donkey serum, 3% bovine serum albumin, 1% gelatin, 0.2% Triton X-100, and 0.2% saponin) at 37°C for 30 minutes and then washed in 1% bovine serum albumin, followed by 0.05% Brij-35, and then incubated overnight at 4°C with murine anti-human MUC5AC IgG1 (diluted 1:500; Chemicon, Billerica, MA) or nonimmune murine IgG to identify cells undergoing mucus metaplasia within the bronchial epithelium. After washing in PBS containing 1% bovine serum

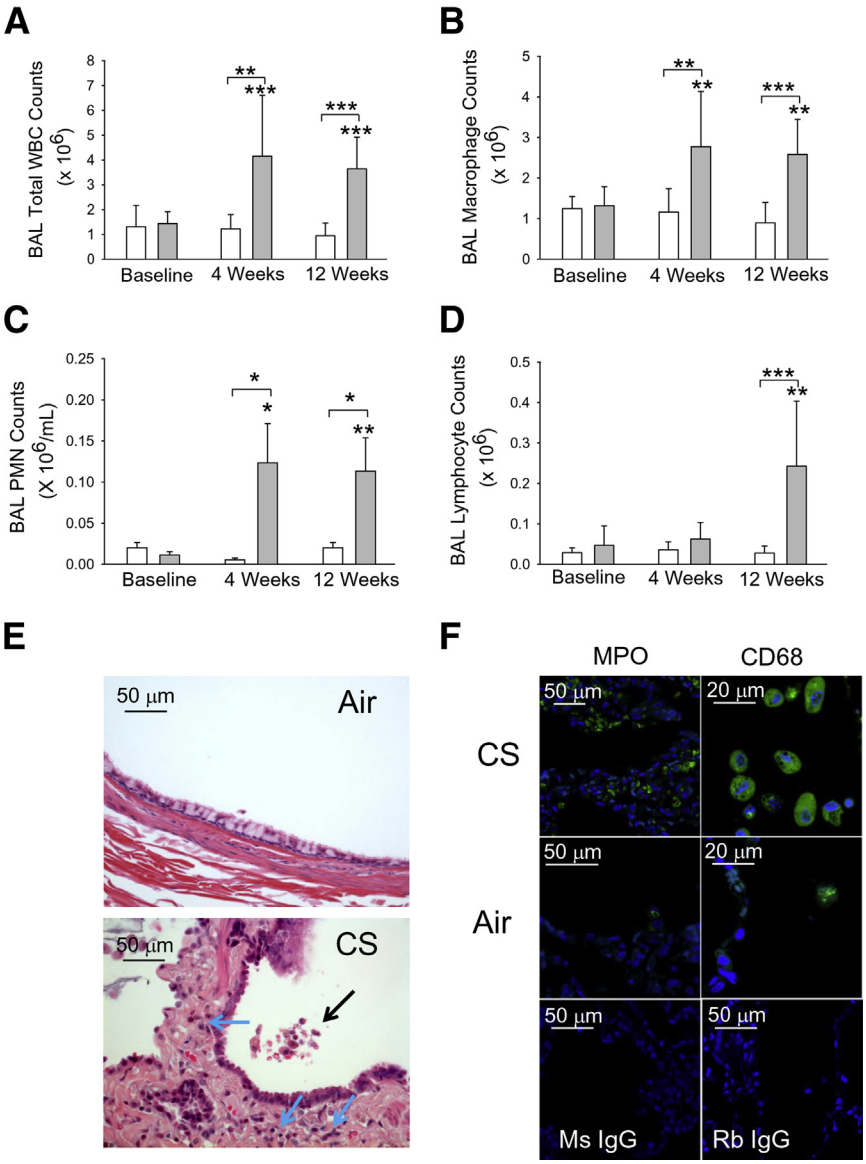

Figure 1 Cigarette smoke (CS) exposure increases bronchoalveolar lavage (BAL) leukocyte counts in nonhuman primates (NHPs). NHPs were exposed to air ($n = 8$; white bars) or CS ($n = 8$; gray bars) for 12 weeks, and BAL was performed at baseline and after 4 and 12 weeks of air or CS exposure. Total and differential leukocyte counts were performed on BAL samples (**top** and **middle panels, F**). **A:** BAL total leukocyte counts. **B:** BAL macrophage counts. **C:** BAL polymorphonuclear neutrophil (PMN) counts. **D:** BAL lymphocyte counts. **E:** Lung sections stained for hematoxylin and eosin from NHPs exposed to air or CS for 12 weeks. The **black arrow** indicates an inflammatory cell infiltrate in the bronchial lumen; **blue arrows**, inflammatory cells infiltrating the airway walls. Images shown in **E** and **F** are representative of five animals per group. **F:** Lung sections from NHPs exposed to CS or air for 12 weeks. Lung sections were immunostained with Alexa 488 and a PMN marker [myeloperoxidase (MPO)] or a macrophage marker (CD68). **Bottom panels:** Lung sections from CS-exposed NHPs immunostained with isotype-matched murine and rabbit control primary IgG antibodies. Data are expressed as means ± SEM (**A**–**D**). $^{*}P < 0.05$, $^{**}P < 0.01$, and $^{***}P \leq 0.001$ versus the group indicated and the same group at baseline (**A**–**D**). Original magnifications: ×300 (MPO staining; **F**); ×500 (CD68 staining; **F**). WBC, white blood cell.

albumin followed by 0.05% Brij, the sections were incubated at 37°C for 1 hour with Alexa 556–conjugated donkey anti-murine IgG diluted 1:300. Sections were then washed in PBS, and nuclei were counterstained with DAPI. Immunofluorescence was imaged using Axioplan 2 (Carl Zeiss, Inc., Thornwood, NY) with a Plan-Neofluor 40×/0.75 air objective and a charge-coupled device camera (Hamamatsu Photonics, Hamamatsu, Japan) with the acquisition software Slidebook 5.0 version 5.0.0.1 (Intelligent Imaging Innovation, Denver, CO).

Submucosal Gland Hyperplasia and Hypertrophy

Lung sections from NHPs exposed to air ($n = 8$) and CS for 4 ($n = 4$) and 12 ($n = 8$) weeks were periodic acid–Schiff stained (as outlined above), and the mean number of submucosal glands was counted in all large cartilaginous bronchi in the tissue sections from each animal. The mean size of the submucosal glands was also quantified using MetaMorph software version 7.7.0.0 (Molecular Devices, Wetzlar, Germany).

Airway and Vessel Remodeling

Extracellular matrix (ECM) protein deposition around small airways and vessels was assessed in paraffin-embedded and formalin-fixed lung sections from NHPs exposed to air or CS for 12 weeks ($n = 5$ per group), stained with Masson's trichrome stain using a commercial kit (Sigma-Aldrich). Large airways were defined as airways having cartilage, whereas small airways were defined by those lacking cartilage. MetaMorph software was used to quantify the mean thickness of the layer of proteins stained blue by Masson's trichrome stain. The area of ECM protein deposited around vessels and airways was quantified in pixels^2 per unit internal circumference of the vessel and per length of the bronchial wall in pixels.

Airspace Measurement

Lungs of NHPs exposed to air or CS for 12 weeks (eight animals per group) were inflated to 25 cm H_2O pressure, removed, fixed in 10% buffered formalin, and paraffin embedded. Lung sections from all of the lobes were cut (5 μm thick), deparaffinized, and stained with hematoxylin and eosin. Digital images of the stained slides were captured using an Olympus NanoZoomer (Hamamatsu Photonics) slide scanner with a 20× objective, and the VisioMorphDP module of VisioPharm analysis software (VisioPharm, Horsholm, Denmark) was used to measure alveolar volume. Volume-weighted mean volumes of alveoli were measured using the method of point-sampled intercepts.[30] This method combines measurements of both mean volume and variability of size of the specified parenchymal airspaces. The volume-weighted mean volumes of alveoli can be estimated on a single section, and the estimation is unbiased without shape assumptions.[31,32]

Oxidative Stress

Thiobarbituric acid—reactive substances (a measure of lipid peroxidation) were measured in homogenates of lung tissue using a commercial kit (Cayman Chemical Company, Ann Arbor, MI) following the manufacturer's instructions. In addition, we performed immunofluorescence staining of peripheral lung sections from NHPs exposed to air or CS for 12 weeks ($n = 4$ per group) with rabbit IgG to human 4-hydroxynonenal (4-HNE; Bioss, Woburn, MA) incubated at 37°C for 1 hour at a 1:50 dilution or nonimmune rabbit IgG as a control. After washing the lung sections with PBS, the sections were incubated at 37°C for 1 hour with Alexa 488—conjugated goat anti-rabbit $F(ab')^2$, diluted 1:100. Sections were then washed in PBS, and nuclei were counterstained with DAPI. Images of the stained lung sections were analyzed using an epifluorescence microscope, as described above.

Alveolar Septal Cell Apoptosis

Alveolar septal cell apoptosis was measured in lung sections from NHPs exposed to air ($n = 4$) or CS ($n = 5$) for 12 weeks using terminal deoxynucleotidyl transferase-mediated dUTP nick-end labeling (TUNEL) staining with an Apoalert DNA Fragmentation Detection Kit (Clontech Laboratories, Mountain View, CA) following the manufacturer's instructions, using TdT terminal transferase—negative TUNEL as control. In addition, we stained lung sections for active (cleaved) caspase-3. Lungs were deparaffinized, and Ag retrieval was performed by heating the slides in a microwave in citrate buffer (see above). The sections were incubated for 1 hour at 37°C with a murine IgG to human active caspase-3 (diluted 1:100; Abcam) or nonimmune murine IgG as control. After washing the lung sections with PBS, the sections were incubated at 37°C for 1 hour with Alexa 488—conjugated goat anti-rabbit $F(ab')^2$, diluted 1:100. Sections were then washed in PBS, and nuclei were counterstained with DAPI. MetaMorph software was used to quantify apoptotic cells for both assays. The number of apoptotic cells was normalized by unit of alveolar wall area.

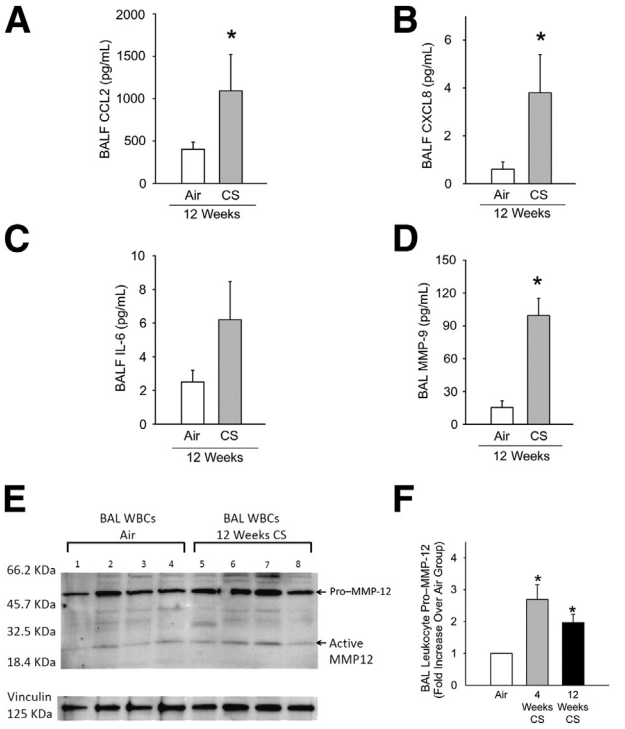

Figure 2 Cigarette smoke (CS) exposure increases inflammatory cytokine and matrix metalloproteinase 9 (MMP-9) levels (but not MMP-12 levels) in nonhuman primate (NHP) bronchoalveolar lavage fluid (BALF) samples, and modestly increases levels of MMP-12 in BAL leukocytes. Levels of chemokine ligand (CCL) 2 (**A**), CXCL8 (**B**), IL-6 (**C**), and MMP-9 (**D**) in BALF samples from NHPs exposed to air or CS for 12 weeks. **C:** There is a trend toward an increase in BALF IL-6 levels in CS-exposed NHPs ($P = 0.1$). **E:** Equal amounts of total protein in BAL leukocyte extracts were subjected to Western blot analysis for MMP-12, and vinculin was used as a loading control. **F:** Quantification of pro—MMP-12 in BAL leukocyte extracts by Western blot analysis. The pro—MMP-12 signals were normalized to signals for a housekeeping protein (vinculin) and expressed as fold change relative to corrected signals in cells from the air-exposed NHPs. Data are for BAL leukocytes isolated from seven NHPs exposed to air, four in NHPs exposed to CS for 4 weeks, and seven NHPs exposed to CS for 12 weeks. Data are presented as means ± SEM (**A**—**D** and **F**). $n = 8$ NHPs per group (**A**—**D**). $^*P < 0.05$ compared with signals in cells from air-exposed NHPs (**A**—**D** and **F**).

Statistical Analysis

Data are presented as means ± SD for continuous variables. Parametric data were analyzed using the Student's *t*-test, whereas the *U*-test was used for nonparametric data. $P < 0.05$ was considered to be statistically significant. Analyses were completed using SigmaStat version 2.03 (Systat Software, San Jose, CA) and GraphPad Prism 6 (GraphPad Software Inc., San Diego, CA).

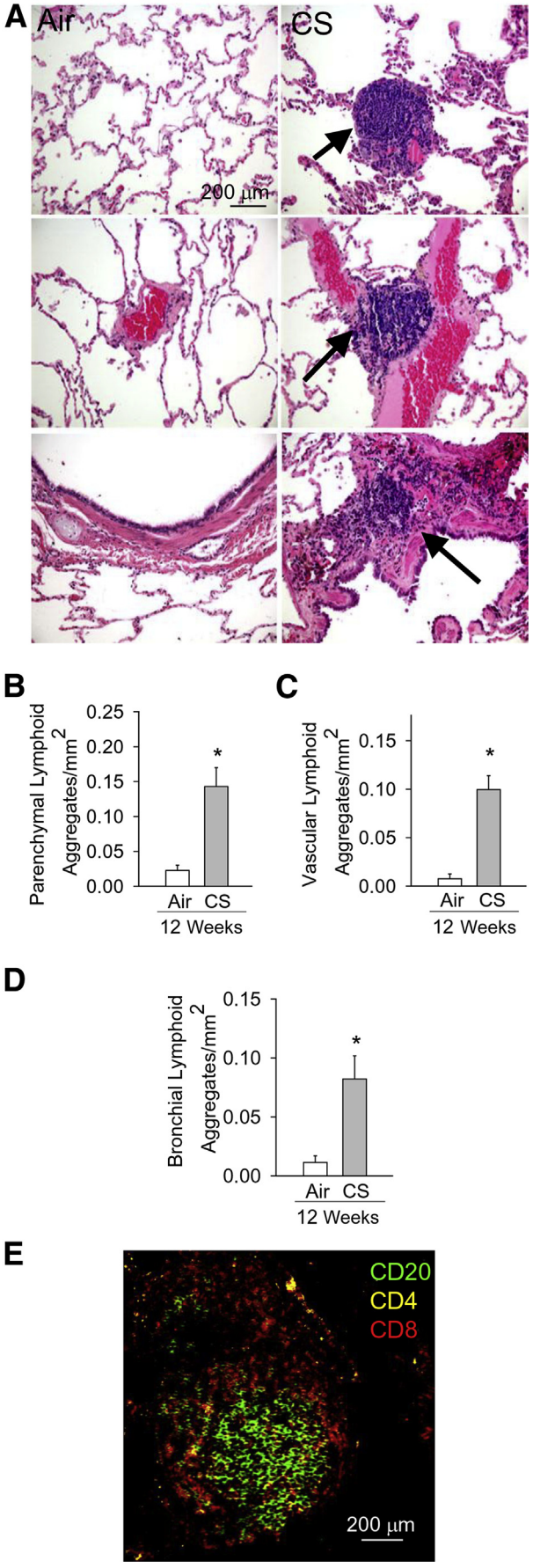

Results

CS Induces Pulmonary Inflammation Detected in BAL Samples in NHPs

We performed an initial experiment to determine whether exposing NHPs to CS versus air for up to 4 weeks results in significant pulmonary inflammation and airway pathologies, including mucus metaplasia, because these events can be detected soon after humans start smoking and long before they develop COPD.[33] In the second experiment, we exposed NHPs to CS or air up to 12 weeks to determine whether longer CS exposures increase pulmonary inflammation and mucus metaplasia further, and to assess whether NHPs exposed to CS for 12 weeks also develop other airway pathologies (small airway remodeling), airspace disease (emphysema), signs of adaptive immune responses (lymphoid aggregates), abnormalities in lung physiology (airflow obstruction and increases in lung compliance), and measures of systemic inflammation characteristic of human COPD.

Exposing NHPs to CS ($n = 8$) resulted in significant increases in total leukocyte counts in BAL samples compared with air-exposed NHPs ($n = 8$) detected as early as 1 week of CS exposure (means ± SEM: $1.7 \pm 0.1 \times 10^6$ versus $1.1 \pm 0.13 \times 10^6$ leukocytes, respectively; $P < 0.005$). Total leukocyte counts increased after 4 weeks and remained elevated after 12 weeks of CS exposure (Figure 1A). The increases in BAL leukocyte counts were due mainly to increases in macrophage counts (Figure 1B). On average, macrophages represented 92% and 70.8% of the BAL leukocytes at baseline and after 12 weeks of CS exposure, respectively. Significant increases in BAL macrophage counts were detected as early as 1 week of CS exposure (means ± SEM: $1.4 \pm 0.1 \times 10^6$ versus $1.0 \pm 0.1 \times 10^6$ macrophages for CS- versus air-exposed NHPs, respectively; $P < 0.05$) in the 4-week exposure study. Significant increases in BAL PMN counts were detected after 4 weeks of CS exposure (Figure 1C). On average, PMNs represented 0.76% and 2.9% of BAL leukocytes at baseline and after 4 weeks of CS exposure, respectively. BAL PMN counts remained elevated after 12 weeks of CS exposure. In contrast, lymphocyte counts did not significantly increase until NHPs

Figure 3 Cigarette smoke (CS) exposure increases lymphoid aggregate counts in nonhuman primate (NHP) lungs. **A:** Hematoxylin and eosin staining of lung sections from NHPs exposed to air or CS for 12 weeks. **Top**, **middle**, and **bottom panels:** Lymphoid aggregates in or around lung parenchyma, vessels, and bronchi, respectively, are indicated by **arrows**. **B**–**D:** Quantitation of lymphoid aggregates in parenchyma (**B**), and around vessels (**C**) and bronchi (**D**) in the lungs of air- and CS-exposed NHPs normalized to the area of the tissue in each microscopic field (30 randomly captured fields per animal). **E:** Triple-color immunofluorescence staining of a lymphoid aggregate in a representative lung section from a CS-exposed NHP. B lymphocytes are identified with a green fluorophore; $CD8^+$ T lymphocytes, a red fluorophore; and $CD4^+$ T lymphocytes, a yellow fluorophore. Data are presented as means ± SEM (**B**–**D**). $n = 7$ NHPs per group (**B**–**D**). *$P < 0.05$ versus the air-exposed NHPs (**B**–**D**). Original magnification, ×400 (**A** and **E**).

had been exposed to CS for 12 weeks (Figure 1D). On average, lymphocytes represented 2.7% and 6.6% of all BAL leukocytes at baseline and after 12 weeks of CS exposure, respectively.

CS Induces the Accumulation of Leukocytes in the Airway Walls and Lumen and the Peripheral Lungs of NHPs

Examination of hematoxylin–eosin–stained lung sections from NHPs exposed to air or CS for 12 weeks revealed infiltration of the airway walls with inflammatory cells along with inflammatory cells in the lumen of the CS-exposed NHPs but no airway inflammation in the lungs of air-exposed NHPs (Figure 1E). When we immunostained lung sections with markers of leukocyte subsets, we observed increased numbers of PMNs (myeloperoxidase-positive cells) and macrophages (CD68-positive cells) in the distal lung parenchyma (Figure 1F) as well as in the airway walls (data not shown) of NHPs exposed to CS when compared to air-exposed animals. There was no staining in lung sections stained with isotype-matched nonimmune control antibodies for either the PMN marker or the macrophage marker.

CS Increases BALF Levels of Proinflammatory Mediators and MMP-9

Levels of CCL2, CXCL8, and IL-6 were measured in BALF samples from NHPs exposed to air and CS for 12 weeks. These cytokines were selected on the basis of their known potent activities in stimulating the recruitment (and/or activation) of monocytes (CCL2 and IL-6) and PMNs (CXCL8 and IL-6) into the CS-exposed lung.[34,35] BALF levels of CCL2 and CXCL8 were significantly increased after 12 weeks of CS exposure (Figure 2, A and B), and there was a strong trend ($P = 0.1$) toward higher BALF levels of IL-6 in CS-exposed NHPs (Figure 2C).

We also compared lung levels of MMP-9 and MMP-12 in BAL samples from air-versus CS-exposed NHPs because MMP-9 is the major MMP released by CS-activated human lung macrophages, whereas MMP-12 is the major MMP released by CS-activated lung macrophages from commonly studied small experimental animals, including mice and guinea pigs.[36] MMP-9 levels were robustly (approximately sixfold) increased in BALF samples after 12 weeks of CS exposure (Figure 2D). In contrast, we did not detect any MMP-12 signals in BALF samples from NHPs exposed to either air or CS for up to 12 weeks using Western blot analysis (data not shown). However, we detected MMP-12 in extracts of BAL leukocytes from NHPs (Figure 2E). The main form detected was pro–MMP-12, and only weak signals corresponding to active MMP-12 were detected in these samples. Pro–MMP-12 levels in BAL leukocytes were increased 2.7-fold after 4 weeks of CS exposure and twofold after 12 weeks of CS exposure when compared with levels in BAL leukocyte air-exposed animals (Figure 2F). Active

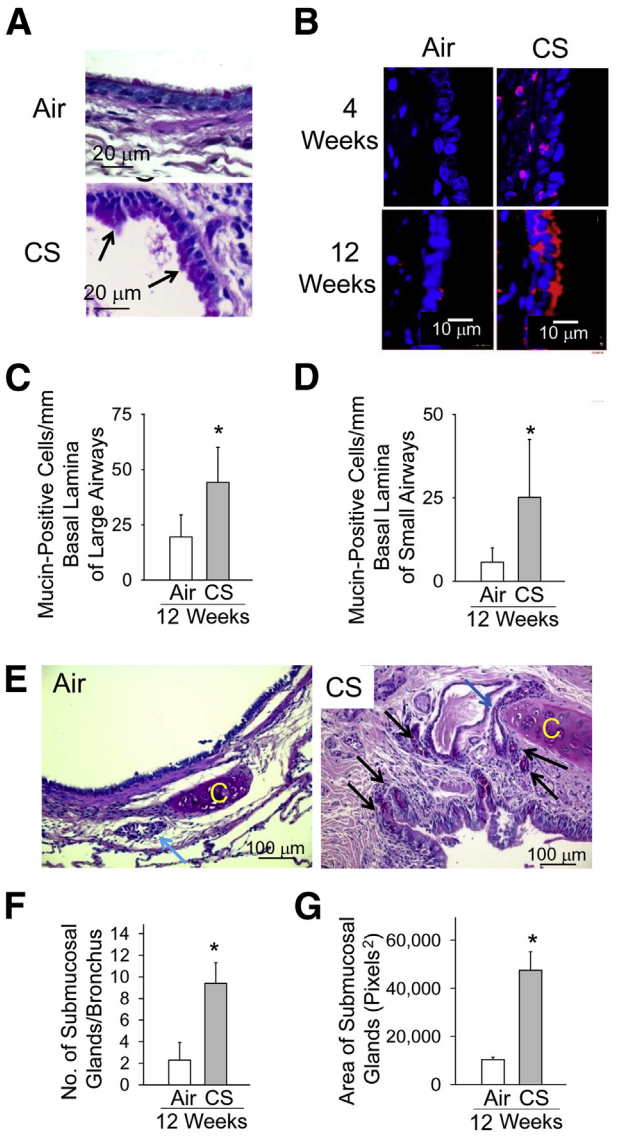

Figure 4 Cigarette smoke (CS) induces mucus metaplasia in large and small airways. Lung sections from nonhuman primates (NHPs) exposed to air or CS for 12 weeks stained with periodic acid–Schiff stain (**A**) or immunostained with a red fluorophore for MUC5AC (**B**). Nuclei were counterstained with DAPI. **C** and **D:** The number of cells undergoing mucus metaplasia in the large (**C**) and small (**D**) airways of NHPs exposed to air ($n = 7$) or CS ($n = 8$) for 12 weeks. **E:** Representative images of the airway submucosal glands in air- and CS-exposed NHPs. The **blue arrow** indicates a larger submucosal gland in the airway of the CS-exposed NHP when compared with the single submucosal gland in the air-exposed NHP; and **black arrows**, hyperplasia of submucosal glands in the CS-exposed NHP. C indicates cartilage present in the large airways. **F** and **G:** The quantitative assessment of the number of submucosal glands per airway and the mean size of submucosal glands in the airways of NHPs exposed to CS ($n = 8$) or air ($n = 8$) for 12 weeks. Data are means ± SEM (**C**, **D**, **F**, and **G**). *$P < 0.05$ compared with air-exposed NHPs (**C**, **D**, **F**, and **G**).

MMP-12 levels in BAL leukocytes from NHPs exposed to CS for 12 weeks were modestly, but significantly, increased (144.5 ± SD 25.3% of levels in cells from air-exposed animals; $P = 0.013$; $n = 4$ NHPs per group) when corrected for vinculin signals (used as a loading control).

CS Increases Lymphoid Aggregate Numbers in NHP Lungs

In addition to increases in numbers of innate immune cell counts in the lungs, human COPD patients develop an adaptive immune response characterized by the formation of lymphoid follicles and aggregates around the airways and in the lung parenchyma.[37,38] NHPs exposed to CS for 12 weeks developed increased numbers of lymphoid aggregates in their lung parenchyma (Figure 3, A and B) and around pulmonary vessels (Figure 3, A and C) and airways (Figure 3, A and D). The lymphoid aggregates were mainly composed of $CD20^+$ B cells and $CD4^+$ T lymphocytes in their centers and $CD8^+$ T lymphocytes in their peripheries (Figure 3E), as reported for lymphoid aggregates/follicles in human COPD lungs.[38]

CS Exposure Induces Mucus Metaplasia in the Large and Small Airways of NHPs

NHP lung sections stained with periodic acid–Schiff stain (Figure 4A) or immunostained for MUC5AC (Figure 4B) revealed that air-exposed NHPs had few airway mucin-expressing cells, but mucus cell metaplasia was readily evident in airway epithelia of NHPs exposed to CS for 4 weeks and increased further after 12 weeks of CS exposure. Mucus cell metaplasia was present in the epithelia of both large (cartilaginous) and small (noncartilaginous) bronchi in the CS-exposed animals (Figure 4, C and D, respectively). In addition, NHPs exposed to CS for 12 weeks had increases in submucosal glands in their large airways (Figure 4E), including submucosal gland hyperplasia (Figure 4F) and submucosal gland hypertrophy (Figure 4G).

CS Exposure Induces Small Airway and Vessel Remodeling in NHPs

Masson's trichrome staining of lung sections revealed increased deposition of ECM proteins around small (non-cartilaginous) bronchi (Figure 5, A and C) and small vessels (Figure 5, B and D) in the lungs of NHPs exposed to CS for 12 weeks. The deposition of ECM proteins around airways and vessels was also present (albeit not as severe) in the lung of NHPs exposed to CS for 4 weeks (data not shown).

CS Does Not Cause Airspace Enlargement in NHPs

In addition to airway disease, airspace enlargement is a common pathology in human COPD lungs and contributes to the airflow obstruction that is characteristic of human COPD.[39] However, NHPs did not develop significant airspace enlargement after 12 weeks of CS exposure (means ± SEM alveolar space area for CS-exposed NHPs: $4.90 \times 10^6 \pm 0.53 \times 10^6$ μm^2 versus $4.39 \times 10^6 \pm 0.43 \times 10^6$ μm^2 for air-expose NHPs). Nevertheless, distal lung pathologies that contribute to emphysema development, including pulmonary inflammation (vide supra) and oxidative stress and alveolar septal cell apoptosis (vide infra), were affected by 12 weeks of CS exposure.[7]

CS Increases Oxidative Stress in NHP Lungs

NHPs exposed to CS for 12 weeks had increased lung levels of thiobarbituric acid–reactive substances (a measure of lipid peroxidation)[40] (Figure 6A) when compared with NHPs exposed to air for 12 weeks. To identify the cells that produce reactive oxygen species or reactive nitrogen species in the CS-exposed NHP lung, we immunostained lung sections with an antibody to 4-hydroxy-nonenal (4-HNE), which is a major aldehyde product of ω-6-unsaturated fatty acid peroxidation.[41] Robust 4-HNE staining was detected in the lungs of CS-exposed animals mainly in inflammatory cells (Figure 6B) and lymphoid aggregates (Figure 6C), whereas the lungs of air-exposed NHPs showed minimal 4-HNE staining (Figure 6D). Lung sections stained with isotype-matched nonimmune control antibodies showed no staining (Figure 6E).

CS Increases Alveolar Septal Cell Apoptosis in NHPs

The number of TUNEL-positive (Figure 7, A and B) and active (cleaved) caspase 3–positive (Figure 7, C and D)

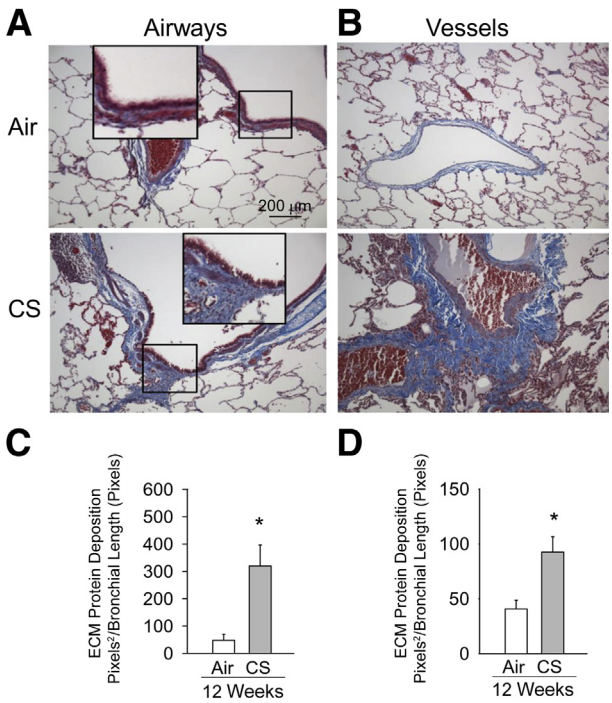

Figure 5 Cigarette smoke (CS) induces extracellular matrix (ECM) protein deposition around small airways and vessels in nonhuman primate (NHP) lungs. **A** and **B:** Lung sections from NHPs exposed to air or CS for 12 weeks immunostained with Masson's trichrome stain to visualize deposition of ECM proteins (visualized as blue staining) around small airways (**A**) and vessels (**B**) of NHPs exposed to CS for 12 weeks compared with NHPs exposed to air. **C** and **D:** Quantitation of ECM protein deposition around bronchi and small vessels, respectively, in air- and CS-exposed animals normalized to the length of the bronchial wall or the length of the vessel internal circumference, respectively. Data are means + SEM (**C** and **D**). $n = 5$ NHPs per group (**C** and **D**). *$P < 0.05$ versus air-exposed animals (**C** and **D**). Original magnification, ×200 (**A** and **B**).

cells was significantly increased in the alveolar septae of NHPs exposed to CS for 12 weeks when compared with that in air-exposed animals. Few apoptotic cells were detected after 4 weeks of CS exposure (data not shown).

PFTs in CS-Exposed NHPs

Exposure of NHPs to CS caused no statistically significant effects on PFT results during the 12-week study period. CS exposure did not affect quasistatic compliance, forced vital capacity, or individual measures of forced expiratory flows (Table 2) (data not shown). The forced expiratory volume in 0.1 seconds was similar in the air- and CS-exposed groups at baseline and at the 4-week time point. However, after 12 weeks of CS exposure, there was a strong trend toward lower forced expiratory volume in 0.1 seconds in the CS- versus air-exposed NHPs ($P = 0.088$) (Table 2). Also, NHPs exposed to air for 12 weeks had a small decrease in mean chord compliance (7.6% reduction), whereas NHPs exposed to CS had a 20% increase in mean chord compliance (data not shown).

CS Does Not Induce Loss of Body Weight or a Systemic Inflammatory Response in NHPs

NHPs exposed to CS did not have significant loss of body weight over the 12-week exposure period (data not shown). We also did not detect significant changes in serum levels of IL-6, CCL2, CXCL8, or MMP-9 in NHPs after 4 or 12 weeks of CS exposure when compared with air-exposed NHPs (data not shown).

Discussion

We show, for the first time, that CS-exposed NHPs develop changes in their airways that are similar to those occurring in human COPD patients, including the following: i) airway inflammation, ii) large and small airway mucus metaplasia, iii) airway submucosal gland hypertrophy and hyperplasia, iv) the development of lymphoid aggregates around the airways, and v) small airway fibrosis. Thus, CS-exposed NHPs develop more robust airway pathologies than CS-exposed mice for 12 weeks. Unlike CS-exposed small animals, our study shows that CS-exposed NHPs can safely undergo longitudinal BAL sampling. Thus, CS-exposed NHPs can serve as a useful large animal model of human COPD airway pathologies. CS-exposed NHPs may also be useful for serial sampling for COPD biomarker studies and studies of therapeutics targeting mucus hypersecretion and/or small airway remodeling.

Small Airway and Vessel Remodeling

Small airway remodeling is an important cause of airflow obstruction in COPD patients.[37,42] We now report that exposing NHPs to CS produces robust deposition of ECM proteins around small airways. It is likely that these airway

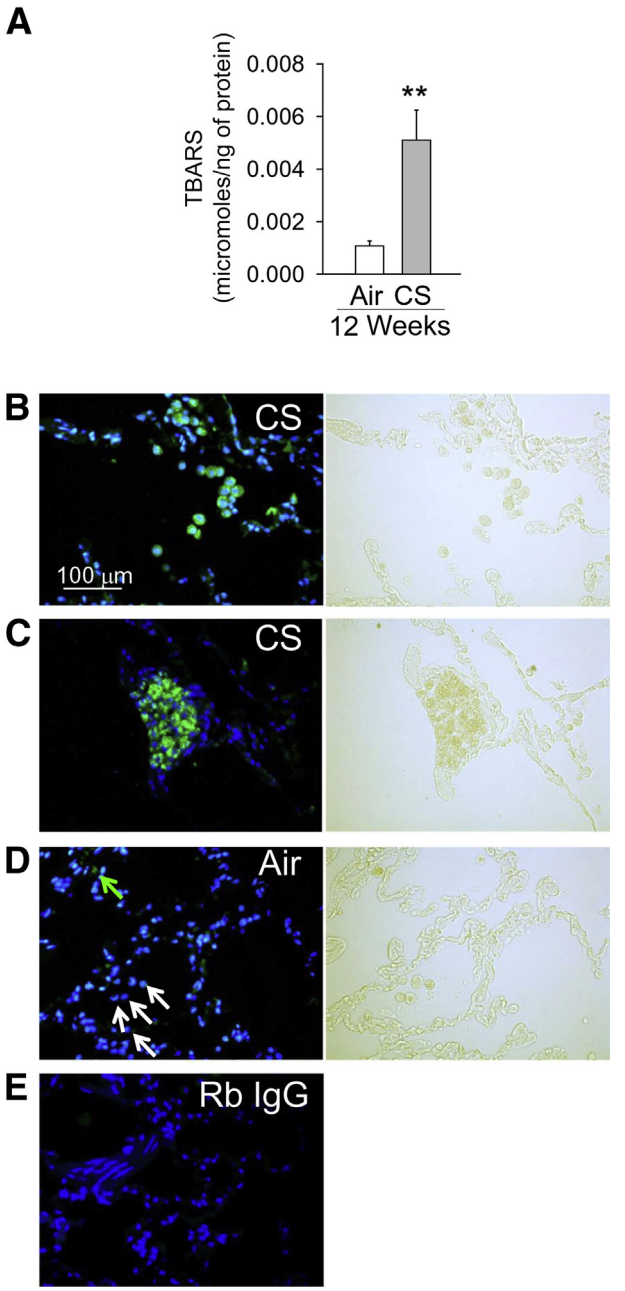

Figure 6 Cigarette smoke (CS) increases oxidative stress levels in nonhuman primate (NHP) lungs. NHPs were exposed to air or CS for up to 12 weeks. **A:** Thiobarbituric acid—reactive substances (TBARS, expressed as micromoles of TBARS per nanogram of protein) were measured in whole lung samples from air- and CS-exposed animals. **B—D:** A representative lung section immunostained for 4-hydroxynonenal (4-HNE) from NHPs exposed to CS (**B** and **C**) or air (**D**) for 12 weeks and the corresponding bright-field images. Intense staining for 4-HNE is detected in lung inflammatory cells (**B**) and lymphoid aggregates (**C**) in the lung of CS-exposed NHPs identified in the bright-field images. Staining for 4-HNE is detected in only a few resident lung macrophages in air-exposed NHPs. **D: Green arrow** indicates a 4-HNE—stained macrophage; and **white arrows**, 4-HNE—negative macrophages. Images shown are representative of those from four NHPs per group. **E:** An image of a lung section stained with a rabbit non-immune control primary antibody. Data are presented as means ± SEM (**A**). $n = 8$ air-exposed animals and $n = 7$ CS-exposed animals per group (**A**). $^{**}P < 0.01$ versus the air-exposed NHPs (**A**). **B—E:** Nuclei were counterstained with DAPI. Original magnification, ×200 (**B—E**). Rb, rabbit.

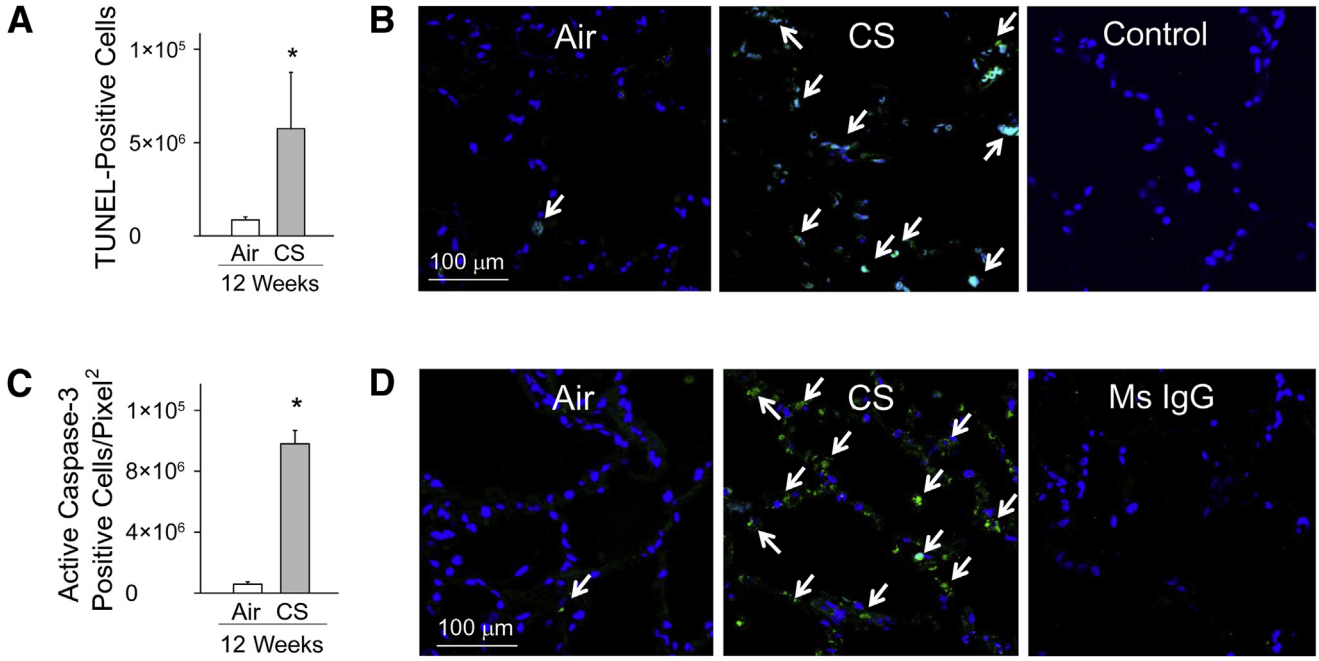

Figure 7 Cigarette smoke (CS) exposure induces alveolar septal cell apoptosis in peripheral lung. Nonhuman primates (NHPs) were exposed to air or CS for 12 weeks, and terminal deoxynucleotidyl transferase-mediated dUTP nick-end labeling (TUNEL) staining was performed on formalin-fixed lung sections. **A:** Quantification of TUNEL-positive cells in air- and CS-exposed groups normalized to unit area of the alveolar wall. **B, top panels:** Representative images of TUNEL staining of lung sections from air- and CS-exposed NHPs. **Arrows** indicate TUNEL-positive cells. **B, bottom panel:** Lung sections from CS-exposed NHPs that were subjected to TUNEL staining with the terminal deoxynucleotidyl transferase (TdT) enzyme omitted as a negative control. **C:** Quantification of active caspase-3–positive alveolar septal cells in air- and CS-exposed NHP lungs normalized to area of lung tissue. **D, top panels:** Representative images of active caspase-3 staining in the lungs of air- and CS-exposed NHPs. **Arrows** indicate active caspase-3–positive cells. **D, bottom panel:** Lung sections from CS-exposed NHPs immunostained with isotype-matched murine (Ms) control primary IgG antibody. Data are presented as means ± SEM (**A** and **C**). $n = 4$ air-exposed NHPs and $n = 5$ CS-exposed NHPs per group (**A**); $n = 5$ NHPs per group (**C**). $^*P < 0.05$ versus air-exposed NHPs (**A** and **C**). Original magnification, ×600 (**D**).

changes contributed to the trend toward the reductions in forced expiratory volume in 0.1 seconds (a readout of airflow obstruction) observed in CS-exposed NHPs. Mice require 24 weeks of CS exposure before they develop relatively mild airway fibrosis,[43] whereas NHPs develop robust small airway remodeling after only 12 weeks of CS exposure. The extent of the small airway ECM protein deposition is greater in CS-exposed NHPs than mice (3 versus 1.5-fold increases, respectively[43,44]). Prior studies have reported thickened basement membranes and smooth muscle hypertrophy in allergen-exposed NHPs,[45–47] and chronic respiratory bronchiolitis associated with restricted airflow in ozone-exposed NHPs.[48] Interestingly, we also detected fibrosis around the small vessels in CS-exposed NHPs, which has not been reported previously in NHP models of airway disease.

Mucus Metaplasia

Mucus hypersecretion due to mucus metaplasia and submucosal gland hypertrophy and hyperplasia[19] occurs in COPD patients, and predisposes patients to the development of acute exacerbations.[49] A major limitation of CS-exposed mice as a COPD model system is that mice lack submucosal glands, have few goblet cells, and only develop mild airway mucus cell metaplasia after 24 weeks of CS exposure.[3] However, CS-exposed NHPs developed impressive hyperplasia and some hypertrophy of bronchial submucosal glands, and extensive mucus metaplasia both in their large cartilaginous and noncartilaginous airways within 4 weeks of CS exposure. These results suggest that CS-exposed NHPs are a useful model system for testing novel therapeutics for mucus hypersecretion.

Lung Inflammation

NHPs exposed to CS had increases in lung myeloid leukocyte counts similar to those seen in COPD patients. Macrophages (an important culprit in human COPD[50]) were the main leukocyte subset increased in the CS-exposed NHP lungs, as reported for other CS-exposed animals, including mice. PMNs also play a key role in the pathogenesis of human COPD by promoting destruction of the alveolar walls during emphysema development via their complement of serine proteinases and MMPs.[51] Although PMNs represent only a small percentage of the BAL leukocytes in CS-exposed mice,[52] lung PMN counts increased approximately 12-fold in CS-exposed NHPs. We also detected increases in BALF levels of mediators that recruit and activate these myeloid leukocytes in the lung (CCL2, CXCL8, and IL-6). Lung

Table 2 Lung Function of NHPs in Response to CS Exposure

Lung function	Air	CS
$FEV_{0.1}$ (mL)		
Baseline	50 (5.6)	50 (10.4)
4 Weeks	46 (12)	45 (9.4)
12 Weeks	43 (12.5)	33 (9)*
Cst (mL/cm H_2O)		
Baseline	13 (3.5)	10 (5)
4 Weeks	11.6 (3)	11.5 (5.2)
12 Weeks	12 (2.4)	12 (5)

Pulmonary function testing using whole-body plethysmography was performed on NHPs at baseline and after 4 and 12 weeks of air or CS exposure. Data are presented as means ± SEM. $n = 8$ NHPs per group.

*Trend toward lower $FEV_{0.1}$ in NHPs exposed to CS for 12 weeks compared with NHPs exposed to air for 12 weeks ($P = 0.088$).

CS, cigarette smoke; Cst, quasistatic compliance calculated from the lung volume-pressure flow curves; $FEV_{0.1}$, forced expiratory volume in 0.1 seconds; NHP, nonhuman primate.

inflammatory responses to injury in NHPs have not been well studied previously. However, NHPs infected with *Bacillus anthracis* develop robust systemic and pulmonary inflammation, and lung injury associated with high mortality.[53]

We found impressive increases in MMP-9 levels in BALF samples, which were likely derived from activated macrophages (as well as epithelial cells and PMNs in the lung[54–56]). However, we did not detect MMP-12 in BALF samples in any animal tested, even after 12 weeks of CS exposure, and MMP-12 levels increased only modestly in BAL leukocyte extracts from CS-exposed NHPs. Activated macrophages from humans and mice differ in the profiles of MMPs that they produce, with MMP-9 being the main MMP produced by human cells, whereas MMP-12 is the major MMP produced by murine macrophages.[36] Thus, from the expression profile of MMPs that we detected in BALF samples, CS-exposed NHPs more closely resemble human COPD patients than CS-exposed mice.

Adaptive Immunity

CS-exposed NHPs also had evidence of activation of adaptive immune responses, with increases in BAL lymphocyte counts and lymphoid aggregates in the airways and lung parenchyma that were mainly composed of mature B lymphocytes and $CD4^+$ and $CD8^+$ T lymphocytes. Increased numbers of lymphoid follicles or aggregates are present in both the small airways and the peripheral lungs of patients with severe COPD[37] and CS-exposed mice,[57] and lymphoid follicles have been strongly implicated in the pathogenesis of COPD.[57] In CS-exposed mice, the number of aggregates is significantly higher after 6 months than 2 or 4 months of CS exposure.[58] However, NHPs developed eightfold increases in lung lymphoid aggregate counts after only 12 weeks of CS exposure. The antigenic stimuli that trigger the formation of B-cell follicles in COPD patients include microbial Ags,[58] Ags in CS,[38,59] proteolytic fragments of ECM proteins,[60] and epithelial neo-Ags.[61] However, the antigenic stimuli that caused the development of lymphoid aggregates in CS-exposed NHPs were not identified in our study. Whether the activated B cells and $CD4^+$ T cells in these follicles collaborate to generate autoantibodies that amplify lung inflammation and destruction in NHPs, as occurs in COPD patients,[60,62–64] will be the focus of future studies.

Airspace Size

We did not observe airspace enlargement in the CS-exposed NHPs. Likely, significantly >12 weeks of CS exposure is required for NHPs to develop emphysema. It was not possible for us to expose NHPs to CS for periods >12 weeks because of the prohibitively high costs associated with these CS exposure durations. However, CS-exposed NHPs developed increases in three key lung processes that lead to the development of emphysema: pulmonary inflammation (vide supra) and lung oxidative stress levels and rates of alveolar septal cell apoptosis (vide infra).

Oxidative Stress

NHPs exposed to CS had robust increases in lung oxidative stress levels localized mainly to leukocytes in the parenchyma and lymphoid aggregates. CS contains oxidizing toxicants and, when inhaled, induces the release of reactive oxygen species and reactive nitrosylated species by activated PMNs, macrophages, and epithelial cells in the lungs.[7,65] Reactive oxygen species and reactive nitrogen species can injure lung ECM proteins either directly or indirectly by activating latent MMPs and/or inactivating proteinase inhibitors to thereby promote proteolytic destruction of the alveolar walls.[7,39,66]

Alveolar Septal Cell Apoptosis

This process also contributes to the loss of alveolar walls in COPD patients.[67] In mice and rats treated with vascular endothelial growth factor receptor antagonists, apoptosis of alveolar endothelial or epithelial cells is sufficient to cause pulmonary emphysema in the absence of lung inflammation.[67,68] Alveolar septal cell apoptosis was detected in CS-exposed NHPs likely in both type I and type II alveolar epithelial cells on the basis of analysis of bright-field images of the lung sections. CS itself and CS-induced lung inflammation may have contributed to the alveolar septal cell apoptosis observed in CS-exposed NHPs.

Limitations of the Study

The major limitation of our study is that emphysema did not develop in CS-exposed NHPs, and it is likely that CS exposures for >12 weeks would be needed to induce emphysema development in NHPs. Also, the pathological changes observed in NHPs exposed to CS were uniform between

animals, whereas many human cigarette smokers do not develop COPD, and in human smokers who develop COPD, the lung pathologies that develop vary considerably from patient to patient. Thus, although CS-exposed NHPs are a better model system of COPD airway disease than CS-exposed rodents, NHPs still have limitations as a model system for human COPD. Using NHPs to model CS-induced airway disease is also expensive because of the high costs associated with purchasing, housing, and exposing NHPs to CS. There are also ethical issues associated with animal research. Recently, research institutions in the United States have begun the process to limit NHP research activities after heightened concerns about threats from animal rights activists directed against scientists performing primate research.[69] However, primates can provide unique insights into disease pathogenesis that cannot be obtained by studying other organisms.

The advantages of using CS-exposed NHPs over CS-exposed mice as a COPD model system include the following: i) the greater genetic, anatomic, histologic, and physiological similarities between NHPs and humans compared with mice and humans; ii) the more robust airway pathologies than develop in CS-exposed NHPs than CS-exposed mice; iii) the larger size of NHPs compared with rodents, which permits serial bronchoscopies and pulmonary function measurements to be performed safely with techniques and instruments used in human studies; and iv) serial lung samples obtained from CS-exposed NHPs may be useful for biomarker validation studies for early disease detection in cigarette smokers. The greater similarity between NHPs and humans may also make CS-exposed NHPs a good model system for assessing the efficacy (and toxicities) of new therapies under controlled conditions before clinical trials are conducted in humans, in whom variable responses are generally obtained because of differences in ethnicity, smoking history, drug use, and comorbidities.

Acknowledgments

The study was performed at Division of Pulmonary and Critical Care Medicine, Brigham and Women's Hospital, Harvard Medical School (Boston, MA) and The Lovelace Respiratory Research Institute (Albuquerque, NM).

References

1. Murray CJ, Lopez AD: Measuring the global burden of disease. N Engl J Med 2013, 369:448–457
2. Murray CJ, Lopez AD: Alternative projections of mortality and disability by cause 1990-2020: global Burden of Disease Study. Lancet 1997, 349:1498–1504
3. Churg A, Cosio M, Wright JL: Mechanisms of cigarette smoke-induced COPD: insights from animal models. Am J Physiol Lung Cell Mol Physiol 2008, 294:L612–L631
4. March TH, Green FH, Hahn FF, Nikula KJ: Animal models of emphysema and their relevance to studies of particle-induced disease. Inhal Toxicol 2000, 12(Suppl 4):155–187
5. Plopper CG, Hyde DM: The non-human primate as a model for studying COPD and asthma. Pulm Pharmacol Ther 2008, 21:755–766
6. Mestas J, Hughes CC: Of mice and not men: differences between mouse and human immunology. J Immunol 2004, 172:2731–2738
7. Owen CA: Proteinases and oxidants as targets in the treatment of chronic obstructive pulmonary disease. Proc Am Thorac Soc 2005, 2:373–385
8. Herfs M, Hubert P, Poirrier AL, Vandevenne P, Renoux V, Habraken Y, Cataldo D, Boniver J, Delvenne P: Proinflammatory cytokines induce bronchial hyperplasia and squamous metaplasia in smokers: implications for chronic obstructive pulmonary disease therapy. Am J Respir Cell Mol Biol 2012, 47:67–79
9. Martorana PA, Beume R, Lucattelli M, Wollin L, Lungarella G: Roflumilast fully prevents emphysema in mice chronically exposed to cigarette smoke. Am J Respir Crit Care Med 2005, 172:848–853
10. Takahashi S, Nakamura H, Seki M, Shiraishi Y, Yamamoto M, Furuuchi M, Nakajima T, Tsujimura S, Shirahata T, Nakamura M, Minematsu N, Yamasaki M, Tateno H, Ishizaka A: Reversal of elastase-induced pulmonary emphysema and promotion of alveolar epithelial cell proliferation by simvastatin in mice. Am J Physiol Lung Cell Mol Physiol 2008, 294:L882–L890
11. Nyunoya T, March TH, Tesfaigzi Y, Seagrave J: Antioxidant diet protects against emphysema, but increases mortality in cigarette smoke-exposed mice. COPD 2011, 8:362–368
12. Rennard SI, Fogarty C, Kelsen S, Long W, Ramsdell J, Allison J, Mahler D, Saadeh C, Siler T, Snell P, Korenblat P, Smith W, Kaye M, Mandel M, Andrews C, Prabhu R, Donohue JF, Watt R, Lo KH, Schlenker-Herceg R, Barnathan ES, Murray J: The safety and efficacy of infliximab in moderate to severe chronic obstructive pulmonary disease. Am J Respir Crit Care Med 2007, 175:926–934
13. Calverley PM, Sanchez-Toril F, McIvor A, Teichmann P, Bredenbroeker D, Fabbri LM: Effect of 1-year treatment with roflumilast in severe chronic obstructive pulmonary disease. Am J Respir Crit Care Med 2007, 176:154–161
14. Fabbri LM, Calverley PM, Izquierdo-Alonso JL, Bundschuh DS, Brose M, Martinez FJ, Rabe KF: Roflumilast in moderate-to-severe chronic obstructive pulmonary disease treated with longacting bronchodilators: two randomised clinical trials. Lancet 2009, 374:695–703
15. Wright JL, Churg A: Cigarette smoke causes physiologic and morphologic changes of emphysema in the guinea pig. Am Rev Respir Dis 1990, 142:1422–1428
16. Snider GL, Lucey EC, Stone PJ: Animal models of emphysema. Am Rev Respir Dis 1986, 133:149–169
17. Coffman RL, Hessel EM: Nonhuman primate models of asthma. J Exp Med 2005, 201:1875–1879
18. Tyler WS, Tyler NK, Last JA, Gillespie MJ, Barstow TJ: Comparison of daily and seasonal exposures of young monkeys to ozone. Toxicology 1988, 50:131–144
19. Cosio MG, Guerassimov A: Chronic obstructive pulmonary disease: inflammation of small airways and lung parenchyma. Am J Respir Crit Care Med 1999, 160:S21–S25
20. Polverino F, Doyle-Eisele M, McDonald J, Kelly E, Wilder J, Mauderly J, Divo M, Pinto-Plata V, Celli B, Tesfaigzi Y, Owen CA: A novel non-human primate model of cigarette-smoke induced chronic obstructive pulmonary disease (abstract). Am J Respir Crit Care Med 2014, B45. COPD:pathogenesis. May 1, 2014, A2997.
21. Mucha L, Stephenson J, Morandi N, Dirani R: Meta-analysis of disease risk associated with smoking, by gender and intensity of smoking. Gend Med 2006, 3:279–291
22. March TH, Wilder JA, Esparza DC, Cossey PY, Blair LF, Herrera LK, McDonald JD, Campen MJ, Mauderly JL, Seagrave J: Modulators of cigarette smoke-induced pulmonary emphysema in A/J mice. Toxicol Sci 2006, 92:545–559
23. Committee for the Update of the Guide for the Care and Use of Laboratory Animals: National Research Council: Guide for the Care and Use of Laboratory Animals: Eighth Edition. Washington, DC, National Academies Press, 2011

24. Ganesan S, Comstock AT, Kinker B, Mancuso P, Beck JM, Sajjan US: Combined exposure to cigarette smoke and nontypeable Haemophilus influenzae drives development of a COPD phenotype in mice. Respir Res 2014, 15:11
25. Lee KM, Renne RA, Harbo SJ, Clark ML, Johnson RE, Gideon KM: 3-Week inhalation exposure to cigarette smoke and/or lipopolysaccharide in AKR/J mice. Inhal Toxicol 2007, 19:23−35
26. Weissmann N, Lobo B, Pichl A, Parajuli N, Seimetz M, Puig-Pey R, Ferrer E, Peinado VI, Dominguez-Fandos D, Fysikopoulos A, Stasch JP, Ghofrani HA, Coll-Bonfill N, Frey R, Schermuly RT, Garcia-Lucio J, Blanco I, Bednorz M, Tura-Ceide O, Tadele E, Brandes RP, Grimminger J, Klepetko W, Jaksch P, Rodriguez-Roisin R, Seeger W, Grimminger F, Barbera JA: Stimulation of soluble guanylate cyclase prevents cigarette smoke-induced pulmonary hypertension and emphysema. Am J Respir Crit Care Med 2014, 189:1359−1373
27. Finch GL, Lundgren DL, Barr EB, Chen BT, Griffith WC, Hobbs CH, Hoover MD, Nikula KJ, Mauderly JL: Chronic cigarette smoke exposure increases the pulmonary retention and radiation dose of 239Pu inhaled as 239PuO2 by F344 rats. Health Phys 1998, 75:597−609
28. Mauderly JL: Respiratory function responses of animals and man to oxidant gases and to pulmonary emphysema. J Toxicol Environ Health 1984, 13:345−361
29. Knolle MD, Nakajima T, Hergrueter A, Gupta K, Polverino F, Craig VJ, Fyfe SE, Zahid M, Permaul P, Cernadas M, Montano G, Tesfaigzi Y, Sholl L, Kobzik L, Israel E, Owen CA: Adam8 limits the development of allergic airway inflammation in mice. J Immunol 2013, 190:6434−6449
30. Gundersen HJ, Jensen EB: Stereological estimation of the volume-weighted mean volume of arbitrary particles observed on random sections. J Microsc 1985, 138:127−142
31. Hyde DM, Tyler NK, Plopper CG: Morphometry of the respiratory tract: avoiding the sampling, size, orientation, and reference traps. Toxicol Pathol 2007, 35:41−48
32. Fehrenbach A, Ochs M, Wittwer T, Cornelius J, Fehrenbach H, Wahlers T, Richter J: Stereological estimation of the volume weighted mean volumes of alveoli and acinar pathways in the rat lung to characterise alterations after ischaemia/reperfusion. J Anat 1999, 194(Pt 1):127−135
33. Kim V, Kelemen SE, Abuel-Haija M, Gaughan JP, Sharafkaneh A, Evans CM, Dickey BF, Solomides CC, Rogers TJ, Criner GJ: Small airway mucous metaplasia and inflammation in chronic obstructive pulmonary disease. COPD 2008, 5:329−338
34. de Boer WI, Sont JK, van SA, Stolk J, van Krieken JH, Hiemstra PS: Monocyte chemoattractant protein 1, interleukin 8, and chronic airways inflammation in COPD. J Pathol 2000, 190:619−626
35. Yasuda N, Gotoh K, Minatoguchi S, Asano K, Nishigaki K, Nomura M, Ohno A, Watanabe M, Sano H, Kumada H, Sawa T, Fujiwara H: An increase of soluble Fas, an inhibitor of apoptosis, associated with progression of COPD. Respir Med 1998, 92:993−999
36. Churg A, Zhou S, Wright JL: Series "matrix metalloproteinases in lung health and disease": matrix metalloproteinases in COPD. Eur Respir J 2012, 39:197−209
37. Hogg JC, Chu F, Utokaparch S, Woods R, Elliott WM, Buzatu L, Cherniack RM, Rogers RM, Sciurba FC, Coxson HO, Pare PD: The nature of small-airway obstruction in chronic obstructive pulmonary disease. N Engl J Med 2004, 350:2645−2653
38. Polverino F, Baraldo S, Bazzan E, Agostini S, Turato G, Lunardi F, Balestro E, Damin M, Papi A, Maestrelli P, Calabrese F, Saetta M: A novel insight into adaptive immunity in chronic obstructive pulmonary disease: B cell activating factor belonging to the tumor necrosis factor family. Am J Respir Crit Care Med 2010, 182:1011−1019
39. Owen CA: Roles for proteinases in the pathogenesis of chronic obstructive pulmonary disease. Int J Chron Obstruct Pulmon Dis 2008, 3:253−268
40. Puente-Maestu L, Tejedor A, Lazaro A, de MJ, Alvarez-Sala L, Gonzalez-Aragoneses F, Simon C, Agusti A: Site of mitochondrial reactive oxygen species production in skeletal muscle of chronic obstructive pulmonary disease and its relationship with exercise oxidative stress. Am J Respir Cell Mol Biol 2012, 47:358−362
41. Schneider C, Porter NA, Brash AR: Routes to 4-hydroxynonenal: fundamental issues in the mechanisms of lipid peroxidation. J Biol Chem 2008, 283:15539−15543
42. Pare PD, Wiggs BR, James A, Hogg JC, Bosken C: The comparative mechanics and morphology of airways in asthma and in chronic obstructive pulmonary disease. Am Rev Respir Dis 1991, 143:1189−1193
43. Churg A, Tai H, Coulthard T, Wang R, Wright JL: Cigarette smoke drives small airway remodeling by induction of growth factors in the airway wall. Am J Respir Crit Care Med 2006, 174:1327−1334
44. Churg A, Zhou S, Preobrazhenska O, Tai H, Wang R, Wright JL: Expression of profibrotic mediators in small airways versus parenchyma after cigarette smoke exposure. Am J Respir Cell Mol Biol 2009, 40:268−276
45. Schelegle ES, Gershwin LJ, Miller LA, Fanucchi MV, Van Winkle LS, Gerriets JP, Walby WF, Omlor AM, Buckpitt AR, Tarkington BK, Wong VJ, Joad JP, Pinkerton KB, Wu R, Evans MJ, Hyde DM, Plopper CG: Allergic asthma induced in rhesus monkeys by house dust mite (Dermatophagoides farinae). Am J Pathol 2001, 158:333−341
46. Tran MU, Weir AJ, Fanucchi MV, Murphy AE, Van Winkle LS, Evans MJ, Smiley-Jewell SM, Miller L, Schelegle ES, Gershwin LJ, Hyde DM, Plopper CG: Smooth muscle development during postnatal growth of distal bronchioles in infant rhesus monkeys. J Appl Physiol (1985) 2004, 97:2364−2371
47. Evans MJ, Fanucchi MV, Baker GL, Van Winkle LS, Pantle LM, Nishio SJ, Schelegle ES, Gershwin LJ, Miller LA, Hyde DM, Plopper CG: The remodelled tracheal basement membrane zone of infant rhesus monkeys after 6 months of recovery. Clin Exp Allergy 2004, 34:1131−1136
48. Eustis SL, Schwartz LW, Kosch PC, Dungworth DL: Chronic bronchiolitis in nonhuman primates after prolonged ozone exposure. Am J Pathol 1981, 105:121−137
49. Burgel PR,, Wedzicha JA: Chronic cough in chronic obstructive pulmonary disease: time for listening? Am J Respir Crit Care Med 2013, 187:902−904
50. Barnes PJ: Alveolar macrophages as orchestrators of COPD. COPD 2004, 1:59−70
51. Quint JK, Wedzicha JA: The neutrophil in chronic obstructive pulmonary disease. J Allergy Clin Immunol 2007, 119:1065−1071
52. D'hulst AI, Vermaelen KY, Brusselle GG, Joos GF, Pauwels RA: Time course of cigarette smoke-induced pulmonary inflammation in mice. Eur Respir J 2005, 26:204−213
53. Stearns-Kurosawa DJ, Lupu F, Taylor FB Jr, Kinasewitz G, Kurosawa S: Sepsis and pathophysiology of anthrax in a nonhuman primate model. Am J Pathol 2006, 169:433−444
54. Owen CA, Hu Z, Barrick B, Shapiro SD: Inducible expression of tissue inhibitor of metalloproteinases-resistant matrix metalloproteinase-9 on the cell surface of neutrophils. Am J Respir Cell Mol Biol 2003, 29: 283−294
55. Atkinson JJ, Lutey BA, Suzuki Y, Toennies HM, Kelley DG, Kobayashi DK, Ijem WG, Deslee G, Moore CH, Jacobs ME, Conradi SH, Gierada DS, Pierce RA, Betsuyaku T, Senior RM: The role of matrix metalloproteinase-9 in cigarette smoke-induced emphysema. Am J Respir Crit Care Med 2011, 183:876−884
56. Watson AM, Benton AS, Rose MC, Freishtat RJ: Cigarette smoke alters tissue inhibitor of metalloproteinase 1 and matrix metalloproteinase 9 levels in the basolateral secretions of human asthmatic bronchial epithelium in vitro. J Investig Med 2010, 58:725−729
57. Bracke KR, Verhamme FM, Seys LJ, Bantsimba-Malanda C, Cunoosamy DM, Herbst R, Hammad H, Lambrecht BN, Joos GF, Brusselle GG: Role of CXCL13 in cigarette smoke-induced lymphoid follicle formation and chronic obstructive pulmonary disease. Am J Respir Crit Care Med 2013, 188:343−355
58. van der Strate BW, Postma DS, Brandsma CA, Melgert BN, Luinge MA, Geerlings M, Hylkema MN, van den Berg A, Timens W,

Kerstjens HA: Cigarette smoke-induced emphysema: a role for the B cell? Am J Respir Crit Care Med 2006, 173:751–758
59. Koethe SM, Kuhnmuench JR, Becker CG: Neutrophil priming by cigarette smoke condensate and a tobacco anti-idiotypic antibody. Am J Pathol 2000, 157:1735–1743
60. Lee SH, Goswami S, Grudo A, Song LZ, Bandi V, Goodnight-White S, Green L, Hacken-Bitar J, Huh J, Bakaeen F, Coxson HO, Cogswell S, Storness-Bliss C, Corry DB, Kheradmand F: Antielastin autoimmunity in tobacco smoking-induced emphysema. Nat Med 2007, 13:567–569
61. Feghali-Bostwick CA, Gadgil AS, Otterbein LE, Pilewski JM, Stoner MW, Csizmadia E, Zhang Y, Sciurba FC, Duncan SR: Autoantibodies in patients with chronic obstructive pulmonary disease. Am J Respir Crit Care Med 2008, 177:156–163
62. Packard TA, Li QZ, Cosgrove GP, Bowler RP, Cambier JC: COPD is associated with production of autoantibodies to a broad spectrum of self-antigens, correlative with disease phenotype. Immunol Res 2013, 55:48–57
63. Núñez B, Sauleda J, Antó JM, Julià MR, Orozco M, Monsó E, Noguera A, Gómez FP, Garcia-Aymerich J, Agusti A: Anti-tissue antibodies are related to lung function in chronic obstructive pulmonary disease. Am J Respir Crit Care Med 2011, 183:1025–1031
64. Taraseviciene-Stewart L, Burns N, Kraskauskas D, Nicolls MR, Tuder RM, Voelkel NF: Mechanisms of autoimmune emphysema. Proc Am Thorac Soc 2006, 3:486–487
65. Macnee W, Rahman I: Is oxidative stress central to the pathogenesis of chronic obstructive pulmonary disease? Trends Mol Med 2001, 7:55–62
66. Mahadeva R, Shapiro SD: Chronic obstructive pulmonary disease * 3: experimental animal models of pulmonary emphysema. Thorax 2002, 57:908–914
67. Kasahara Y, Tuder RM, Taraseviciene-Stewart L, Le Cras TD, Abman S, Hirth PK, Waltenberger J, Voelkel NF: Inhibition of VEGF receptors causes lung cell apoptosis and emphysema. J Clin Invest 2000, 106:1311–1319
68. Tuder RM, Kasahara Y, Voelkel NF: Inhibition of vascular endothelial growth factor receptors causes emphysema in rats. Chest 2000, 117:281S
69. Garbarini N: Primates as a model for research. Dis Model Mech 2010, 3:15–19